

## Enhanced main chamber wall interaction as an explanation for anomalous divertor detachment on TCV

M. Wischmeier<sup>1</sup>, R.A. Pitts<sup>1</sup>, J. Horacek<sup>1</sup>, D. Coster<sup>2</sup>, D. Reiter<sup>3</sup>

<sup>1</sup> Centre de Recherches en Physique des Plasmas, Association EURATOM-Confédération Suisse, Ecole Polytechnique Fédérale de Lausanne, CH-1015 Lausanne, Switzerland

<sup>2</sup> Max-Planck-Institut für Plasmaphysik, EURATOM-Association, D-85748 Garching, Germany

<sup>3</sup> FZJ-Forschungszentrum Jülich, Association EURATOM-FZJ, D-52425 Jülich, Germany

### Introduction

Tokamak divertor detachment, expected to play a major role in reactor grade devices, is still not completely understood. Only with complex codes such as the coupled version B2.5-EIRENE (SOLPS5.0) [1], used here, can the relative importance of the well known components determining the final detached state be quantified. Confrontation of the results of SOLPS5.0 modeling with experimental data in both deuterium and pure helium plasmas has indicated a relationship between main chamber wall (MCW) interaction and impurity production which provides a possible explanation for the anomalous detachment that has long been observed at the outer target of TCV SNL ohmic discharges.

### Experiment

The open divertor geometry of TCV is shown in Fig. 1 in the form of the grid used for the code simulations, formed by an inner vertical target and an outer horizontal target on the vessel floor with highly asymmetric parallel connection lengths of  $\sim 2.5m$  for the X-point to inner target distance and  $\sim 25m$  (at  $I_p = 340kA, B_T = 1.4T, \kappa \sim 1.65, \delta \sim 0.35$ ) from the outer midplane to the outer target. Prior to the installation of graphite armour on the low field side (LFS), divertor detachment had *never* been observed at the outer target in ohmic density ramp discharges with the  $\vec{B} \times \nabla B$  ion drift directed upward and with pure deuterium fuelling only [2]. Detachment at the inner target is almost never obtained. Detailed observations of the detached regime in TCV may be found in [3, 4]. Both high recycling and detachment at the outer target are found to behave 'anomalously', with the ion saturation current,  $j_{SAT}$ , steadily decreasing with increasing line averaged density,  $\bar{n}_e$ , for target densities  $> 4 \times 10^{19} m^{-3}$ .

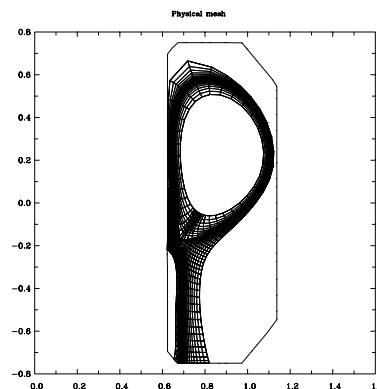


Figure 1: Grid used for the TCV simulations based on the reconstruction of the magnetic equilibrium for the discharge #24532.

At high  $\bar{n}_e$ , tomographic reconstruction of the total radiated power for discharge (#17823) [3,5] shows that most of the power is radiated above the X-point outside the separatrix and only  $\sim 1/3$  of the power reaches the divertor volumes. The possible explanation is that significant impurity sources may be present in the main chamber region.

The influence of field direction: The possible influence of drifts on the detachment threshold has been tested by comparing identical discharges in forward (FWD-B) and reversed (REV-B) toroidal field. Due to the lower L-H transition threshold with favorable ion  $\vec{B} \times \nabla B$  drift, discharges with  $I_p \geq 280kA$  in FWD-B transit to an H-mode at any reasonable density. Good pairs of matched forward and reversed field density ramp and constant  $\bar{n}_e$  discharges have therefore only been obtained in both field directions for  $I_p = 260kA$ .

Fig. 2 shows the integral target ion current for REV-B at  $I_p = 340kA$  and for REV-B, FWD-B at  $260kA$ . Whilst drifts may promote a slightly earlier onset, the detachment itself appears to be largely independent of field direction for the same plasma current.

Helium discharges: In pure *He* density ramp discharges the density limit is  $\sim 15\%$  higher than in *D* at the standard  $I_p = 340kA$ . With increasing  $\bar{n}_e$ , detachment at the outer target is not observed. Fig. 3 compares the

very similar experimental outer target  $j_{SAT}$  profiles at low density obtained in *He* and *D*, whilst Fig. 4 shows how in *D* the outer target is detached at high density but remains attached in *He*. Well matched  $n_e$  and  $T_e$  profiles have been obtained upstream in *D* and *He*, measured by a Thomson scattering system at the top of the poloidal cross-section optimised for edge parameters and a fast reciprocating probe (RCP) located at the tokamak outer midplane. Due to problems with the foil bolometer diagnostic a poloidal reconstruction of the total radiated power for these specific *He* discharges is unfortunately unavailable.

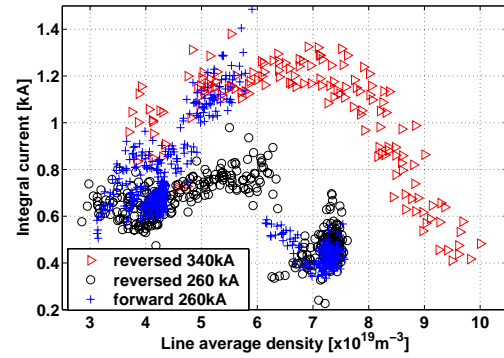


Figure 2: Density dependence of the integral current at the outer target for deuterium density ramp discharges at  $260kA$  in FWD-B (#24395, #26797, #26814) and at  $260kA$  (#24459, #26953, #26814) and  $340kA$  (#24532).

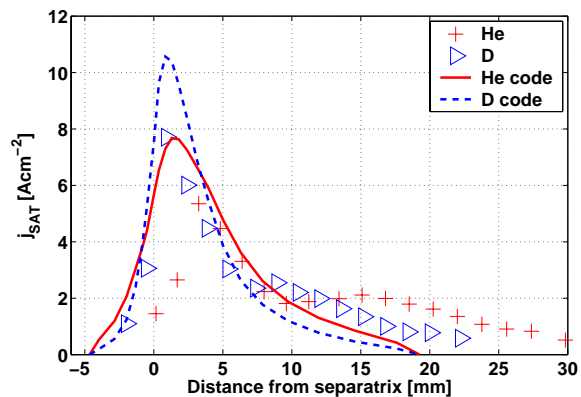


Figure 3: Comparing experimental profiles of  $j_{SAT}$  mapped to outer midplane in *He* (#26212) and *D* (#26979) at low density ( $\bar{n}_e \approx 3.5 \times 10^{19} m^{-3}$ ) with simulations of *He* (11050) and *D* (8524) plasmas.

## Simulation

Early modelling attempts, using the SOLPS4 code package, did not reproduce the detachment in  $D$  plasmas at the outer target without recourse to artificial means such as increasing the coefficient for 3-body and radiative recombination by a factor 5 [4, 5]. In the simulations the plasma (ions) interact with the vessel surfaces only at the divertor targets.

In contrast the EIRENE code does simulate the interaction of neutrals with *all* vessel surfaces. The impurity release due to these neutrals should therefore be correctly accounted for. In the baseline simulations results shown in Fig. 3, the chemical sputtering yield,  $Y_{chem}$ , has been fixed at 3.5% at all surfaces independent of the impinging flux or surface temperature. Using spatially constant transport coefficients ( $D_{\perp} = 0.2m^2s^{-1}$  for  $D$ ,  $D_{\perp} = 0.5m^2s^{-1}$  for  $He$ ,  $\chi_{\perp} = 1.0m^2s^{-1}$  for both) good agreement

between upstream, inner and outer target simulated plasma profiles ( $j_{SAT}$ ,  $n_e$ ,  $T_e$ ) and experimental data (Fig. 3) is obtained for attached plasmas at low densities ( $\bar{n}_e < 4 \times 10^{19}m^{-3}$ ). At higher densities, however, the experimentally observed detachment in  $D$  cannot be reproduced using a simple description of constant transport coefficients and the baseline atomic physics package within SOLPS5. In addition, the upstream  $T_e$  and  $n_e$  profiles cannot be matched. Moreover, neither a refinement of the atomic and molecular physics model for processes involving  $D$  or  $D_2$  (i.e. treatment of vibrationally excited molecules as individual species) nor an increase in  $Y_{chem}$  to any reasonable value at the targets result in a reduction (similar to [6]) of the simulated  $j_{SAT}$  [4]. Including MAR processes in the simulations yielded no evidence for target ion flux detachment.

Radial intermittent transport has been observed in the TCV SOL using the LFS RCP in plasmas with identical configuration to those discussed here [7]. This ‘‘bursty’’ transport increases linearly with the local SOL density. To include this new physics in the simulations an enhanced particle flux,  $\Gamma_{\perp}$ , is imposed as a convective term (similar to the Ansatz in [8]) at high  $\bar{n}_e$ , limited to the SOL on the LFS between the top right corner of the grid and the X-point (see Fig. 1), such that now  $\Gamma_{\perp} = n v_{\perp} + D_{\perp} \nabla n$ . Including this new presentation for the perpendicular flux, reasonable agreement is found between neutral pressure measurements obtained using an ASDEX type fast pressure gauge at the outer midplane and code results. Experimental upstream  $n_e$  and  $T_e$  profiles are also well matched at high  $\bar{n}_e$ . In  $He$  plasmas reasonable agreement is obtained upstream even without imposing a convective de-

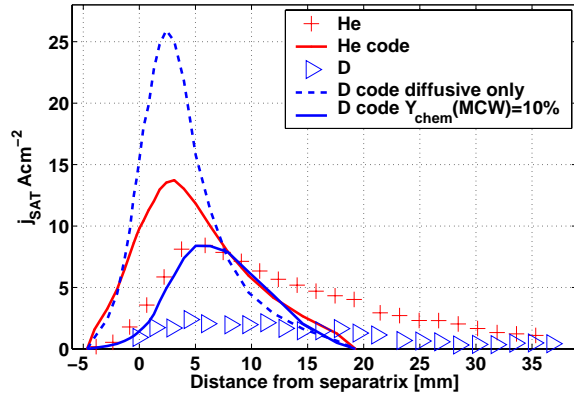


Figure 4: Comparing experimental profiles in  $He$  (#26222) and  $D$  (#24532) at high densities with simulations of  $He$  (11150) and  $D$  plasmas without (8006) and with (10841) enhanced MCW interaction.

scription of the anomalous  $\Gamma_{\perp}$ . The increased MCW recycling flux implied by the enhanced outward convection also implies that carbon impurity release from MCW will also increase, due mostly to chemical sputtering which has no energy threshold. Indeed the fraction of main chamber radiation observed at high density can only be satisfactorily modelled if  $Y_{chem}$  at the MCW is increased to 10% to account for the fact that ion-MCW interactions are not correctly modelled by SOLPS5, Table 1. As shown in Fig. 4 the increased impurity production due to enhanced  $\Gamma_{\perp}$  for high  $\bar{n}_e$  at the MCW results in a drastic decrease of the simulated  $j_{SAT}$ , with values close in the strike point vicinity being as low as in experiment. Sensitivity studies of  $Y_{chem}$  on the MCW and the value of  $P_{SOL}$  show that ohmic detachment on TCV occurs in a narrow operational window. Self-consistent simulations including  $CD_4$  (and its full catabolic chain down to  $D$  and  $C$  products in EIRENE) as a chemically sputtered species instead of the usual description in which atomic  $C$  is released, show the strongest decrease of the simulated  $j_{SAT}$ . The lack of proper accounting of the detailed distribution of the plasma-wall interaction makes it impossible to achieve agreement between model and experiment along the entire outer target. Likewise, it is not yet possible to determine whether MAR involving  $CD_4$  [9] is of importance in further reducing  $j_{SAT}$ .

## Conclusions

Deuterium detachment at the outer target of TCV SNL plasmas can only be simulated if enhanced MCW interaction is accounted for as a consequence of strong intermittent perpendicular transport on the LFS of the plasma cross-section at high density. Only then do the simulations approximately reproduce the experimentally observed distribution of radiated power. In  $He$  plasmas, in which carbon chemical sputtering is absent, impurity production is low at high  $\bar{n}_e$  and agreement is achieved in the simulations without recourse to enhanced MCW interaction. This is supported by the fact that detachment has only naturally been achieved on TCV only since the LFS MCW has been covered by graphite tiles.

*This work was partly funded by the Fonds National Suisse de la Recherche Scientifique.*

## References

- [1] D. P. COSTER et al., *Proc. 19th IAEA Fusion Energy Conference IAEA-CN-94-TH/P2-13* (2002).
- [2] R. A. PITTS et al., *Journal of Nuclear Materials* **266-269**, 648 (1999).
- [3] R. PITTS et al., *Journal of Nuclear Materials* **290-293**, 940 (2001).
- [4] M. WISCHMEIER et al., *Contributions to Plasma Physics* **44**, 268 (2004).
- [5] R. A. PITTS et al., *Proc. 18th IAEA Fusion Energy Conference IAEA-CN-77-EXP/P4-23* (2000).
- [6] U. FANTZ et al., *Journal of Nuclear Materials* **290-293**, 367 (2001).
- [7] J. P. GRAVES et al., *Plasma Phys. Control. Fusion* **47**, L1 (2005).
- [8] A. Y. PIGAROV et al., *Phys. Plasmas* **9**, 1287 (2002).
- [9] R. K. JANEV et al., *Phys. Plasmas* **7**, 4364 (2000).

Experiment	40%
Const. Diff. $Y_{chem} = 3.5\%$	12%
Diff. + Conv., $Y_{chem}(MCW) = 10\%$	46%

Table 1: *Experimental and simulated percentage of SOL radiation above X-pt.*